Journal of Achievements in Materials and Manufacturing Engineering
VOLUME 31
ISSUE 2
December
2008

Torsional fatigue behaviour in gigacycle regime and damage mechanism of the perlitic steel

H.Q. Xue [a,d], E. Bayraktar [b,d,*], I. Marines-Garcia [c,d], C. Bathias [d]

[a] School of Aircraft Design Engineering, Northwestern Polytechnical University, Xi'an China
[b] School of Mechanical and Manufacturing Engineering, EA 2336 Supmeca/LISMMA-Paris, France
[c] Centro de Investigación Sobre Fijación de Nitrógeno, Universidad Nacional Autónoma de México, Cuernavaca, 62210 Morelos, Mexico
[d] Chair of Industrial Materials Laboratory, Conservatoire National des Arts et Métiers, Case 321, Paris, France
* Corresponding author: E-mail address: bayraktar@supmeca.fr

Received 08.09.2008; published in revised form 01.12.2008

Properties

ABSTRACT

Purpose: This paper gives a comprehensive study based on the damage mechanism under torsional fatigue behaviour of D38MSV5S steel in very high cycle regime (VHCF). Torsional fatigue tests have been carried out at 20 kHz ultrasonic fatigue testing device, and these results were compared with that of the conventional torsional fatigue test machine at 35 Hz as to whether the discrepancy due to the frequency effects between two test results. All of the fatigue tests were carried out up to 1010 cycles at room temperature.
Design/methodology/approach: Damage mechanism in torsional fatigues crack initiation and propagation in different mode was evaluated by Scanning Electron Microscopy (SEM).
Findings: The experimental results have shown that the S-N curves exhibited a considerable decrease in fatigue strength beyond 107 cycles.
Practical implications: These results give a precise data for the safety design of the pieces.
Originality/value: Damage mechanism under torsional fatigue loading composes two stages, crack initiation and crack propagation, contrary to the damage under axial loading that exposes only crack initiation mechanism in the VHCF range.
Keywords: Damage mechanisms; Ultrasonic fatigue; Cyclic torsion; Very high cycle range; SEM

1. Introduction

Study of fatigue of the materials extending to fatigue lives in very high cycles (VHCF) regimes (>10^7 cycles) have been performed by a few researchers in the past 20 years to explain fatigue damage mechanism of mechanical parts subjected to the very high vibration. Recent works by using the ultrasonic fatigue devices (20-30 kHz) have shown that many materials, including some steel, aluminium alloy and titanium alloys, intermetallics composites, etc, exhibit a sharp decrease in fatigue strength between fatigue lives of 10^6 and 10^9 cycles [1-16]. So it is necessary to investigate the fatigue behaviour of materials in very high cycle regime. Quite a lot of fatigue investigations in VHCF range of the metallic materials have shown that damage initiate in very high cycle fatigue well below the traditional fatigue limit

© Copyright by International OCSCO World Press. All rights reserved. 2008

explained by the "classical Wöhler S-N curve" [1-35]. For a long time, fatigue damage in VHCF range was explained by internal defects starting from non metallic inclusions. Presently, there seem different ideas on the interpretation of the damage related to the fatigue threshold values in the every stage of fatigue. Even, there are different ideas on the evolution of the S-N curves up to VHCF range. For example Nishijiama [1] and Murakami [2] proposed the variation of the S-N curve by different steps while Bathias [3] and Sakai [4, 5] have shown that there is no fatigue limit in the VHCF ranges. This idea was concluded with a known scientific paper of Bathias [3]; "There is no infinite fatigue life in metallic materials". Recently, Bayraktar et al. [10] have published a paper suggesting that the origin of the internal damage is not only due to inclusions and pores leading to the formation of the fish eye but also due to the slip bands and the nature of the microstructure. For example, two different phases in the microstructure of which mechanical properties are different, causes different behaviour in the same solicitation. They have given also different interpretations on the damage by different internal, subsurface and surface crack initiation types in VHCF range. So; these ideas have been discussing from Paris conference held in 1998 in the frame of "Euromech-382". In fact, the ultrasonic fatigue testing method is not restricted to cyclic axial loading. Today, many engineering components used in modern technology work under combined torsion and axial loading in their working conditions and the cyclic combined loading can result in fatigue fracture after a very long life fatigue regime. For instance, the transmission parts made of structural steel D38MSV5S used in automotive engine [10, 13, 18, 34]. They are subjected to cyclic shear stress and strain under the working conditions However, only a few research groups have carried out ultrasonic torsional fatigue tests in VHCF regime to explain the fatigue properties of materials under ultrasonic torsional cyclic loading [11, 13, 14, 15, 34, 35]. But in our knowledge, there are a few or not sufficient explanations in the literature, on the damage mechanisms under ultrasonic torsional fatigue VHCF range. Knowledge of the materials behaviour under cyclic torsion is of great interest, since loading of several mechanical components is in cyclic torsion rather than cyclic tension–compression. Additionally, Lukas et al. [32] have shown the main differences between low and high cycle fatigue properties. They have proved that plastic deformation in VHCF range is restricted to only one or two grains whereas other grains may stay in a pure elastic range and plasticity occurs mainly in surface grains, which are less constrained than the interior.

In the frame of this study, torsional fatigue properties of D38MSV5S steel (transmission parts made of structural steel D38MSV5S used in automotive engine) have been evaluated that is important alloy used in automotive engine components. As known, these components subjected to low amplitude, high cycle, high frequency cyclic loading in working service. Thus, it is important to examine fatigue behaviour and damage mechanism of these alloys in very high cycle regime. Bayraktar et al [13, 34, 35] have investigated in detail the VHC- fatigue behaviour of different kind of automotive alloys and interpreted damage mechanism in longitudinal loading conditions. Thus, present paper gives attention to only for the pure torsional fatigue testing and the damage mechanisms in VHCF range. Naturally, structural mechanical components subjected to high frequency vibrations, such as those used in rotating parts in engines, are usually required to be designed using a lifetime failure-free criterion for a very large endurance limit. Fatigue data in longitudinal loading are insufficient for assessing VHC- fatigue limit of the components that are subjected to torsional cyclic loading as indicated by Stanzl-Tschegg et al [6]. In the rotating components, fatigue failure occurs under combined bending and torsion l at very high frequency. Thus, it is necessary to investigate the torsion fatigue performance in very high cycle regimes. Since 1993, Stanzl-Tschegg S.E and Mayer [6, 8, 11] designed and constructed an ultrasonic torsional fatigue test system at a frequency of 21 kHz; to investigate torsional fatigue behaviour of alloys. Today, there exists much data in literature for the fatigue behaviour under axial loading in VHCF range, but only a few data can be found for torsional loading in the literature [8, 13, 27, 31, 34]. All of the torsional fatigue tests have been carried out on the new torsional fatigue testing machine at a high frequency of 20 kHz corresponding to fixed numbers of cycles up to 10^{10} cycles that has been developed in the frame of two industrial projects [13, 18]. This torsional testing machine is constructed differently from the machine constructed by Stanzl-Tschegg S.E et al. [6, 8] as will be explained in the following section.

2. Experimental study

2.1. Materials

The microstructure of D38MSV5S steel is shown in Figure 1. It has a ferrito - perlitic structure in which well distribution of micro alloys (Va, Nb) dispersed in the microstructure. Ferrite is about 45% and it contains a very fine inclusions (CaO, Al_2O_3) of about 1μm are distributed in the microstructure. After annealing at 1200°C, it has been cooled in air. The ratio of yield strength and ultimate tensile strength is about 0.7.

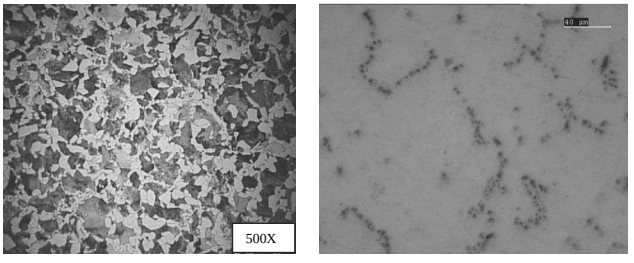

Fig. 1. Microstructure of test alloy (D38MSV5S steel)

2.2. Testing and measurement systems

In order to determine the torsion fatigue limit of the alloy up to 1010 cycles, an ultrasonic torsion fatigue system was designed [8]. The main component of the ultrasonic system is a piezoelectric transducer, which converts an electrical signal at a

frequency of 20 kHz into a mechanical displacement at the same frequency. The electrical signal is fulfilled by a power supply that automatically turns to the natural resonant frequency of the system. Two horns are attached to the transducer; first one should amplify the longitudinal mechanical displacement and second horn is to amplify the torsional angular displacement (Figure 2). In fact, second horn is jointed at the end of the first horn in order to transform the longitudinal displacement to the torsional displacement. A torsion fatigue specimen designed to run in the same resonance with the system and then, this specimen directly attached at the end of the second horn.

In this study, all of the tests have been carried out at a stress ratio of R= –1. Before each test, the strain of specimen is calibrated with a strain gage bonded to the gage section. Under the nominal elastic conditions, a linear relationship is constructed between input displacement and the strain in the gage section for the calibration of the system. The system calibrating result was shown in Figure 3. Thus, automatic test control software continuously can record the displacement and controls the output of the power supply, therefore, indirectly controls the magnitude of the strain in the specimen. This is a basic working principle of the torsional fatigue machine used in this study. All other technical details related to the torsional fatigue system have been published and presented in different journals and symposiums [10, 13, 18, 34].

a)

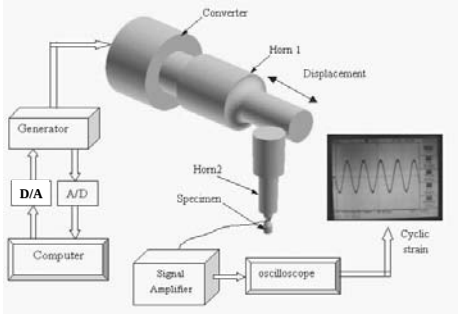

b)

Fig. 2. a) System design of torsional fatigue vibration system and b) testing [10, 13, 18]

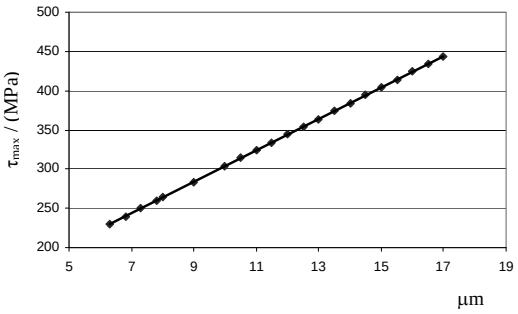

Fig. 3. System calibrating result in cyclic torsion

2.3. Specimen geometry

The specimen geometry of D38MSV5S steel is shown in Figure 4a. The dog-bone shape specimen was designed for this alloy used in ultrasonic torsional fatigue tests so that the maximum strain is located in the gage section as illustrated in Figure 4. Torsional vibration system, the displacement and stress levels during the vibration of specimen is shown in Figures 4b, c and d.

In fact, torsion specimen for an alloy is designed for making to run in the same resonance with the system and the dimension can be determined by analytical or numerical method (ANSYS) depending of the materials properties such as density, Elastic modulus, etc. [7, 9]. Ultrasonic torsional fatigue specimen is considerably smaller than the specimens used for example, tension-compression fatigue testing, since the wavelength of shear waves is smaller.

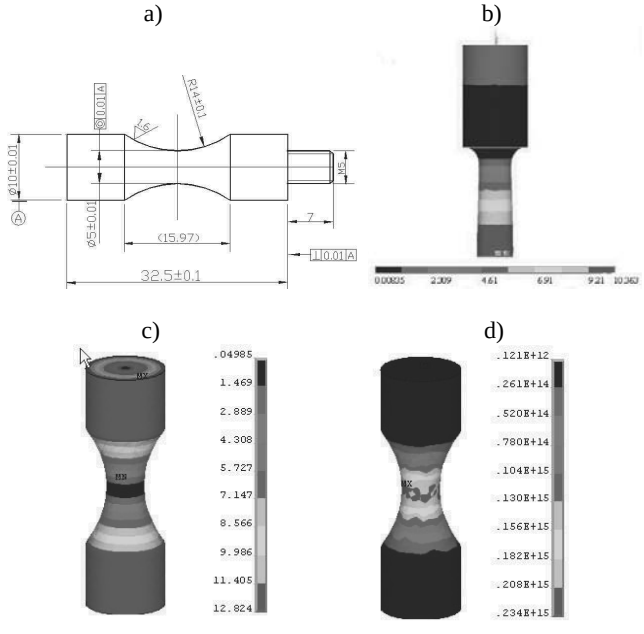

Fig. 4. a) Dimension of D38MSV5S steel specimen, b) torsional vibration, c) displacement and d) stress levels during the vibration of specimen

2.4. Ultrasonic fatigue test programme

Fatigue experiments were conducted on two different fatigue machines, one is a conventional fatigue test machine and the other is the ultrasonic torsional fatigue machine. All of torsional fatigue tests have been carried out at ambient [13, 18] with the stress ratio R = -1 (which is loaded at a frequency of 35 Hz sine - wave loading, and another is ultrasonic fatigue test machine, which 20 kHz sine-loading was applied). In the ultrasonic fatigue system, the specimen is excited to torsion resonance vibration at the ultrasonic frequency of 20 kHz. This leads to torsional shear loading with maximum amplitude in the centre of the specimen. The specimens tested in the ultrasonic fatigue machine were cooled continuously with dry air during fatigue testing to decrease the temperature rise caused by internal friction of material. Failure of the specimens may be detected by monitoring the resonance frequency, which makes possible the automatic operation of the experiments. It means that the test stops automatically when the specimen fails, or it can continue to accomplish 10^{10} cycles.

The staircase method was used to obtain accurate values of the fatigue limit stress for this alloy corresponding to the fixed number of cycles up to 1010 cycles. Before fatigue tests, all specimens had been polished, the roughness of specimen is less than 0.2 μm in order to satisfy and conform to the ASTM standard of fatigue test for metallic materials [8]. Conventional fatigue tests (35 Hz) were conducted on the INSTRON fatigue test machine, which the cycle stress loading were controlled. The conventional fatigue test results were between 104 and 107 cycles and ultrasonic fatigue test results were between 105 and 1010 cycles. The DAS1602 data acquisition device had been applied in recoding the fatigue test results accurately. Control program had been written in C++ language, it controls the data acquisition and fatigue test procedure. Fatigue crack initiation, the microstructure and short cracks in the fatigue specimens were examined using both optical and scanning electron microscopes (SEM). The chemical compositions at the crack initiation site were analysed by an energy disperse spectrometry (EDS).

3. Results and discussion

3.1. Torsional fatigue behaviour and damage mechanism

The "S-N curve" obtained from torsional fatigue tests of D38MSV5S steel was given in Figure 5. Fatigue lifetime increases as the stress amplitude decreases in the life range of 10^4~$2x10^6$ cycles, then stress amplitude decreases slowly. Stress amplitude decreases from 240 MPa to 260 MPa in the range of $2x10^6$-10^{10} cycles. Generally, the evolution of the S-N curve of this alloy is continuously decreasing from the mega to the gigacycle range. Even this curve decreases lightly; the fatigue limit defined by means of a statistical analysis between 106 and 107 cycles can not guarantee for a safe design of the components subjected to very high vibration. These results obtained at different frequency show that there is no evident frequency effect in our experimental conditions.

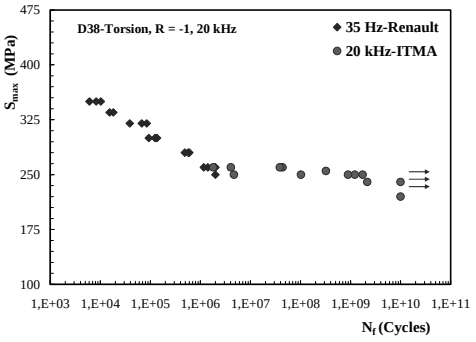

Fig. 5. Torsion fatigue test results of D38MSV5S steel (R=-1)

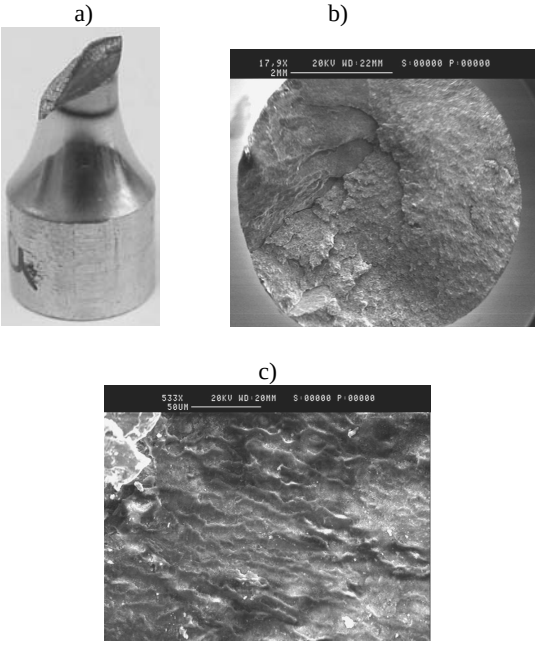

Fig. 6. Torsional fatigue fracture surface τ_{max} =250 MPa, R=-1, N_f=2.09x10^9), a) Overview of the fracture surface, b) shear band in the crack growth region

General observations conducted on the fractured specimen show the well known fatigue mechanisms in torsion [10-12]. Shear crack nucleation is followed by crack growth on the planes where the principal stress amplitude is at maximum. A small crack is nucleated on one of the planes of maximum shear and propagates up to a length of several hundred microns. Then crack branching occurs but only one of these cracks prevails for the final failure of the specimens, and propagating on one of the planes of maximum normal stress. Typical crack patterns observed at the surfaces of the specimens explain that the cracking takes place on the longitudinal plane (i.e. maximum shear plane), with final fracture occurring in a spiral shape on a 45º plane (maximum principal stress plane). Even the failure

crack appeared on the maximum principal stress plane at 45º, the fatigue damage mechanism is always shear type failure.

Fatigue crack initiations have began from the surface of the fractured specimens for the D38MSV5S steel. Figure 6a shows a typical torsion fatigue fracture surface of D38MSV5S steel tested at 20 kHz frequency, at an applied maximum torsional stress level of 250 MPa, with N_f=2.09x10^9 cycles. The crack origin is seen very clearly and crack growth occurs in the 45°of the axial direction and shear step is also very clear in the crack growth region. Evidently, many small shear bands are observed near the fatigue initiation site (Figure 6b). The similar fatigue fracture surface with surface fatigue initiation and apparent shear step and shear fatigue bands have also been observed for all other samples. Another typical sample fractured at stress level of 250 MPa with N_f =3.65x10^7 cycles is presented in Figure 7.

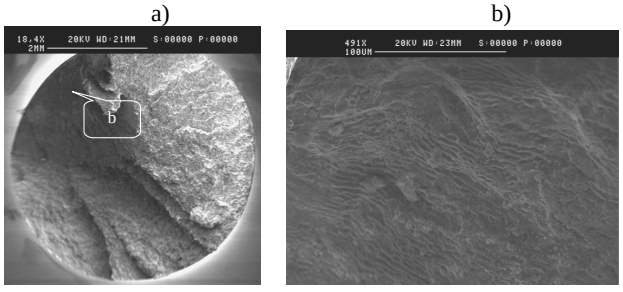

Fig. 7. Torsion fatigue fracture surface of D38MSV5S specimen (τ_{max} =250 MPa, R=-1, N_f = 4.65x10^7); a) overview and b) fatigue shear band in the fatigue initiation zone)

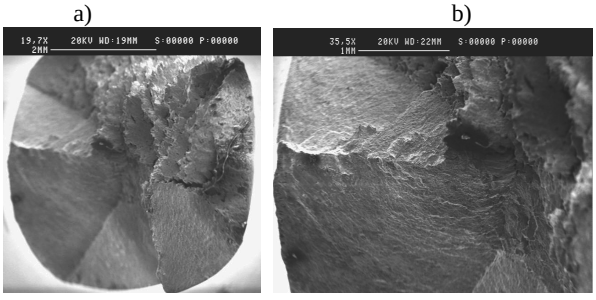

Fig. 8. Torsional fatigue fracture surface of D38MSV5S (τ_{max} =260 Mpa, R=-1, N_f=3.8x10^6); a) overview and b) fatigue shear step

Generally, fatigue fracture surfaces of D38MSV5S steel have indicated that the fatigue initiations begin always from the surface. In other words, fatigue crack initiation and propagation occur on the maximum shear planes and also crack growth plane expose a typical spiral (torsional) form in the 45° fracture plane. Thus, fatigue crack propagates in different shear planes and shear steps occurred in fatigue crack propagation zone. Figure 8 shows another typical torsion fatigue crack growth in a spiral form (45° fracture plane).

Under low cyclic stress, even the bigger shear steps can not be found, the smaller shear steps are very noticeably observed on a spiral 45° fracture plane, as shown in Figure 9a. The higher magnification of the shear step was shown in Figure 9b. Moreover, many micro-cracks around the principle crack are also observed in some of the fractured specimen (Figure 9c). This tendency confirms that fatigue crack initiation occurs always in maximum shear plane and then crack growth is observed in one of the planes of maximum principal stress.

Figure 9c shows simply a secondary crack and Figure 9d indicates that the fatigue crack initiation has began from a surface defect. Fractography in these figures confirm surely that the shear planes are always near the fatigue initiation sites.

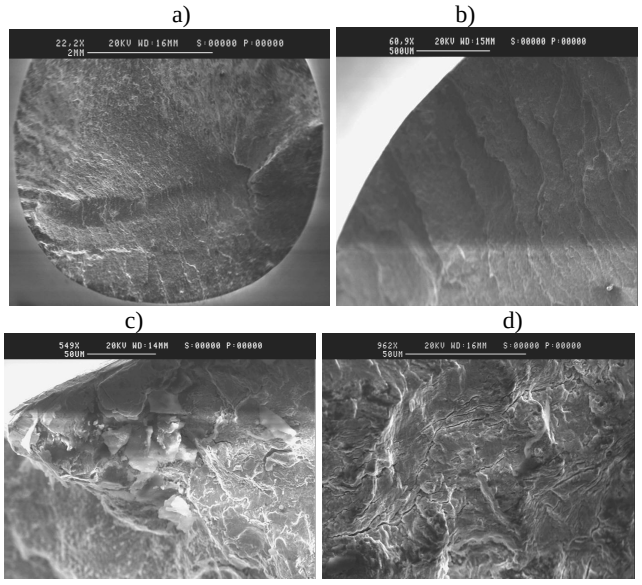

Fig. 9. Torsional fatigue fracture surface of D38MSV5S specimen (τ_{max} =240Mpa, R =-1, N_f=6.9x10^8), a) overview, b) fatigue shear step, c) secondary cracks and d) fatigue initiation

3.2. Mechanism-I: Fatigue crack initiation

For the specimen subjected to torsion cycle loading, the position of the normal and shear stresses is show in Figure 10. Both the tensile and compressive stresses are 45° to the specimen axis and remain mutually perpendicular. One shear stress component is parallel with the specimen axis; the other is perpendicular to the specimen axis. Under a cyclic torsional load, fatigue crack has initiated from the surface of the centre of specimen where subjected to maximum shear stress. When the fatigue crack initiation occurs, the local stress increases, and different states of stress exist around the fatigue crack initiation, and local tensile stress on the 45° plane will exceed largely the tensile strength of the alloys before the local shear stress reaches the shear strength of the alloy. Thus, fracture takes place normal to the 45° tensile plane producing a typical torsional fracture surface as shown in Figure 10. As mentioned also by other researchers, when smooth specimens are subjected to torsional fatigue loading, crack initiation follows to Mode II [20-23]. It

means that crack initiation occurs on the planes where the shear stress amplitude is at maximum level. Even at early stages of the crack propagation on the specimen surface, it follows Mode II [20]. When the shear crack reaches a threshold value, depending on the material characteristics and number of cycle to failure [23], crack branching occurs and crack propagates in the same direction.

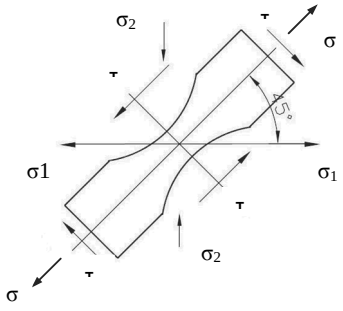

Fig. 10. Schematic presentation of the normal and shear stresses in torsion fatigue specimen

3.3. Mechanism-II: Fatigue crack propagation

Fatigue test results show that the fracture surface exposes apparent shear fatigue strips. The crack propagation was always oriented at approximately 45° to the axis of the specimen. This indicates that final fracture was the origin of the tensile stress normal to the 45° plane and not the shear stress. As known, the shear stress would be expected to cause an overload failure. Additionally, many micro-cracks around a principle crack are observed at only a few fracture surfaces. This tendency indicates that fatigue crack initiation and propagation occur on one of the planes of maximum shear stress. In consequence, the secondary crack can be easily found in the fracture surfaces. The cleavage type fracture surface occurred in the final overload region. Damage mechanism under torsional fatigue loading composes certainly two stages, crack initiation and crack propagation, contrary to the damage under axial loading that exposes only crack initiation mechanism in the VHCF range. This result is the originality of this research. The crack propagation life is longer than the crack initiation life for a solid specimen in cyclic torsion loading. This case is proved evidently many shear strips in fatigue fracture surfaces. This result also is basically contrary to the results obtained under axial loading in VHCF range.

4. Conclusions

Torsional fatigue tests has been carried out for a safe design of the components in the VHCF range for D38MSV5S steel used as a transmission parts in automotive engine. Principal torsional damage analyse based on the test results are presented in this paper. The following conclusions can be summarized:

- Fatigue lifetime increases when the stress amplitude decreases in the range of 10^6~10^{10} cycles for both of alloys subjected to ultrasonic torsional loading.
- Crack initiation appears on one of the maximum shear stress plane for the ductile material. Fatigue crack propagation appears on the maximum principal stress plane. Thus, the fatigue damage mechanism is always shear type failure.
- Fatigue crack initiation of all the fractured specimens for this alloy begins from the surface of the specimens.
- Damage mechanism under torsional fatigue loading composes two stages, crack initiation and crack propagation, contrary to the damage under axial loading that exposes only crack initiation mechanism in the VHCF range.
- The crack propagation life is longer than the crack initiation life for a solid specimen in cyclic torsion loading. This case is proved evidently many shear strips in fatigue fracture surfaces.

Acknowledgements

The authors are grateful to the research managers of RENAULT-FRANCE, ASCOMETAL-FRANCE, and A2M-FRANCE for valuable help during this project, “Predict-I”.

References

[1] S. Nishijiama, K. Kanazawa, Stepwise S-N curve and fish-eye failure in gigacycle regime, Fatigue and Fracture of Engineering Materials and Structures 22 (1999) 601-607.
[2] Y. Murakami, Y. Takada, T. Toriyama, Super-long life tension-compression fatigue properties of quenched and tempered 0.46%C steel, International Journal of Fatigue 16 (1998) 661-667.
[3] C. Bathias, There is no infinite fatigue life in metallic materials, Fatigue and Fracture of Engineering Materials and Structures 22 (1999) 559-565.
[4] T. Sakai, K. Takeda K. Shiozawa, Y. Ochi, M. Nakajima, T. Nakamura, N. Oguma, Experimental evidence of duplex S-N characteristics in wide life region for high strength steels, Proceedings of the 7th International Fatigue Congress “Fatigue’99”, Beijing, 1999, 573-578.
[5] T. Sakai, H. Hirano, T. Nishida, T. Tomoto, A study on ultra long life fatigue characteristics in rotating bending for aluminium alloy with some surface treatments, Proceedings of the 3rd International Conference “Very High Cycle Fatigue” VHCF-3, Kyoto, 2004, 585-592.
[6] S.E. Stanzl-Tschegg, H.R. Mayer, E.K. Tschegg, The influence of air humidity on near-threshold fatigue crack growth of 2024-T3 aluminium alloy, Materials Science and Engineering A 147 (1991) 45-54.
[7] Q.Y. Wang, J.Y. Berand, C. Bathias, Gigacycle fatigue of ferrous alloys, Fatigue and Fracture of Engineering Materials and Structures 22/8 (1999) 667-672.
[8] H. Mayer, M. Papakyriacou, B. Zettl, S.E. Stanzl-Tschegg, Influence of porosity on the fatigue limit of die cast

magnesium and aluminium alloys, International Journal of Fatigue 25 (2003) 245-256.
[9] J. Ryan, M. Nicholas, T. Nicholas, Fatigue strength of Ti–6Al–4V at very long lives, International Journal of Fatigue 27 (2005) 1608-1612.
[10] E. Bayraktar, I.G. Marines, C. Bathias, Failure mechanisms of automotive metallic alloys in very high cycle fatigue range, International Journal of Fatigue 28 (2006) 1590-1602.
[11] S.E. Stanzl-Tschegg, H.R. Mayer, E.K. Tschegg, High frequency method for torsion fatigue testing, Ultrasonics 31/4 (1993) 275-280.
[12] C. Bathias, Piezo-electric fatigue testing machines and devices, Proceedings of the 3rd International Conference "Very High Cycle Fatigue" VHCF-3, Kyoto, 2004, 472-483.
[13] H.Q. Xue, Explanation on gigacycle fatigue of materials in tension, bending and torsion loading, PhD thesis, CNAM, Arts et Métiers, Paris, 2005.
[14] P. Davoli, A. Bernasconi, M. Filippini, S. Foletti, I.V. Papadopoulos, Independence of the torsional fatigue limit upon a mean shear stress, International Journal of Fatigue 25 (2003) 471-480.
[15] D. Mcclaflin, A. Fatemi, Torsional deformation and fatigue hardened steel including mean stress and stress gradient effects, International Journal of Fatigue 26 (2004) 773-784.
[16] A. Varvani-Farahani, T. Kodric, A. Ghahramani, A method of fatigue life prediction in notched and un-notched components, Journal of Materials Processing Technology 169 (2005) 94-102.
[17] H. Mughrabi, On the life-controlling microstructural fatigue mechanisms in ductile metals and alloys in the gigacycle regime, Fatigue and Fracture of Engineering Materials and Structures 22 (1999) 633-641.
[18] I. Marines-Garcia, J.-P. Doucet, C. Bathias, Development of a new device to perform torsional ultrasonic fatigue testing, International Journal of Fatigue 29/9-11 (2007) 2094-2101.
[19] H. Mughrabi, Specific features and mechanisms of fatigue in the ultrahigh cycle regime, Proceedings of the 3rd International Conference "Very High Cycle Fatigue" VHCF-3, Kyoto, 2004, 14-23.
[20] D. Socie, J. Bannantine, Bulk deformation fatigue damage models, Materials Science and Engineering A 103 (1988) 3-13.
[21] G. Marquis, D. Socie, Long-life torsion fatigue with normal mean stresses, Fatigue and Fracture of Engineering Materials and Structures 23 (2000) 293-300.
[22] L. Susmel, D. Taylor, A simplified approach to apply the theory of critical distances to notched components under torsional fatigue loading, International Journal of Fatigue 28 (2006) 417-430.
[23] C. Makabe, D. Socie, Crack growth mechanisms in precraked torsional fatigue specimens, Fatigue and Fracture of Engineering Materials and Structures 24 (2001) 607-615.
[24] H. Mayer, C. Ede, J.E. Allison, Influence of cyclic loads below endurance limit or threshold stress intensity on fatigue damage in cast aluminium alloy 319-T7, International Journal of Fatigue 27 (2005) 129-141.
[25] Q.Y. Wang, J.Y. Berand, C. Bathias, Gigacycle fatigue of ferrous alloys, Fatigue and Fracture of Engineering Materials and Structures 22/8 (1999) 667-672.
[26] C. Bathias, How and why the fatigue S-N curve does not approach a horizontal asymptote, International Journal of Fatigue 23/1 (2001) 143-151.
[27] H. Mayer, Ultrasonic torsion and tension – compression fatigue testing: Measuring principles and investigations on 2024-T351 aluminium alloy, International Journal of Fatigue 28 (2006) 1446-1455.
[28] T. Nomoto, T. Ueda, Y. Murakami, on the mechanisms of fatigue failure in the super long life regime, Fatigue and Fracture of Engineering Materials and Structures 23 (2000) 893-910.
[29] G. Chai, Fatigue behaviour of duplex phase alloys in the very high cycle regime, Proceedings of the 3rd International Conference "Very High Cycle Fatigue" VHCF-3, Kyoto, 2004, 374-381.
[30] T. Nakamura, H. Oguma, et al., Characteristics of initial fatigue crack propagation process of Ti-6Al-4V in very high cycle fatigue, Proceedings of the 3rd International Conference on Very High Cycle Fatigue "VHCF"-3, Kyoto, 2004, 201-208.
[31] H. Mayer, M. Papakyriacou, B. Zettl, S. Vacic, Endurance limit and threshold stress intensity of die cast magnesium and aluminium alloys at elevated temperatures, International Journal of Fatigue 27 (2005) 1076-1088.
[32] P. Lukas, L. Kunz, Specific features of high-cycle and ultra-high-cycle fatigue, Fracture of Engineering Materials and Structures 25 (2002) 747-53.
[33] B. Zettl, H. Mayer, C. Ede, S. Stanzl-Tschegg, Very high cycle fatigue of normalized carbon steels, International Journal of Fatigue 28 (2006) 1583-1589.
[34] H.Q. Xue, E. Bayraktar et al, Torsional fatigue behaviour and damage mechanism of automotive components in VHCF range, Proceeding of the 9th International Fatigue Congress "Fatigue 2006", Atlanta, 2006.
[35] E. Bayraktar, R.P. Mora, I. M. Garcia, C. Bathias, Surface effect on the fatigue behaviour of mechanical components in gigacycle regime, Proceedings of the 4th International Conference "Very High Cycle Fatigue" VHCF-4, Ann Arbor, 2007.